Handling Qualities Considerations in Control Allocation for Multicopters

Christina M. Ivler
Ivler@up.edu
Assistant Professor of Mechanical Engineering

William Hunter
Hunterw21@up.edu
Undergraduate Research Assistant

Emily Vo
Voe22@up.edu
Undergraduate Research Assistant

Kate Russell
Russelk22@up.edu
Undergraduate Research Assistant

Shiley School of Engineering at the University of Portland
Portland, OR

Carlos Malpica
Aerospace Engineer

Shannah Withrow-Maser
Aerospace Engineer

NASA Ames Research Center
Moffett Field, CA

ABSTRACT

Due to multicopters' role in advanced air mobility, there has been an increasing interest in their handling qualities. This paper investigates the effect of rotor speed control allocation of multicopters on handling qualities. Typically, multicopter aircraft are trimmed with equal speed on each rotor. The force generated by each rotor can be modeled, where thrust and torque of the rotor are related to the square of the rotor speed. The dynamic equations indicate that trimming pairs of motors at different speeds results in an increase of control effectiveness in the associated axis, improving bandwidth and disturbance rejection. A tradeoff occurs where power usage is no longer optimized, but handling qualities are improved in that control axis. A blade element model for multicopter, RMAC, was used to simulate how this off-nominal control allocation would affect the dynamics of a multicopter. System identification flight tests were used to validate the trends seen in RMAC. Control systems were optimized to provide improved disturbance rejection bandwidth in the axis associated with increased rotational speed. Unmanned mission task elements were performed in flight test, showing improved tracking in the lateral axis by using off-nominal mixing to increase trim speed on the rolling motors.

NOTATION

d	Rotor diameter
i_a	Motor armature current
I_r	Main rotor rotational moment of inertia
J	Motor/drive system rotational mass moment of inertia
J_{avg}	Frequency domain cost function
J_{mf}	Frequency domain model following cost
K	Motor transformation coefficient
K_e	Motor back-EMF constant (Vs)
L_a	Motor armature inductance
L_{lat}	Roll control derivative
L_p	Roll damping derivative
L_v	Roll speed damping derivative
m	Mass
M_{lon}	Pitch control derivative
M_q	Pitch damping derivative
M_u	Pitch speed damping derivative
n	Number of rotors
N_r	Yaw damping derivative
N_{yaw}	Yaw control derivative
p	Roll angular body rate
q	Pitch angular body rate
Q	Torque
r	Yaw angular body rate
R_a	Motor armature resistance
t	Time
T	Thrust
T_{DN}	Thrust mixing matrix
$T_{\bar{x}_i}$	Thrust to normalized input signal control derivative (per motor)
V	Voltage
V_a	Armature voltage
$\bar{x}_i$	Normalized pulse width modulation input signal for each i motor
Z_{thr}	Heave to throttle control derivative
Z_w	Vertical acceleration to vertical velocity derivative (heave damping)
$Z_{\bar{x}_i}$	Vertical acceleration derivative to normalized input signal

Presented at the Vertical Flight Society's 78th Annual Forum & Technology Display, Ft. Worth, TX, USA, May 10-12, 2022.

δ	Perturbation control input
ζ	Damping ratio
κ	Torque coefficient
λ	Inflow ratio
μ	Thrust coefficient
ω	Motor speed
ω_c	Broken loop crossover frequency
ω_n	Natural frequency
Ω	Rotor speed

ACRONYMS

DRB	Disturbance Rejection Bandwidth
DRP	Disturbance Rejection Peak
CIFER	Comprehensive Identification from FrEquency Responses
ESC	Electronic Speed Control
MCP	Maximum Continuous Power
MTE	Mission Task Element
PWM	Pulse Width Modulation
RMAC	Rensselaer Multicopter Analysis Code
RPM	Revolutions per Minute
UAV	Unmanned Aerial Vehicle
UAS	Unmanned Aircraft System
UP	University of Portland
GM	Gain margin
PM	Phase margin

INTRODUCTION

Multirotor vertical lift aircraft are popular small unmanned aerial system configurations because of their utility and mechanical simplicity. Many of these aircraft are controlled via variable speed on the various rotors, which in turn provides thrust, yaw, pitch and roll to control the aircraft. These aircraft are popular and prove useful in the areas of photography, delivery, surveillance and mapping, largely in the hobby and commercial sector but also in military and police applications. These aircraft tend to be small (<55lbs) and unmanned. Given the advantages of this configuration, including the ability to build in safety via redundancy by the inclusion of additional rotors, much interest in recent years has been generated for using these aircraft in larger manned-sized configurations as well [1, 2, 3, 4].

The simplest variable-speed multicopter configuration, the quadcopter, has two pairs of counter-rotating rotors (for anti-torque). These four variable-speed rotors are sufficient for controlling thrust, yaw, pitch and roll, but provide no redundancy in case of failure. Considering the safety advantages of including additional rotors for redundancy, configurations with 3 or more pairs of counter-rotating rotors are being considered for larger, manned configurations. Since only 4 rotors (2 pairs of counter rotating rotors) are required to control the aircraft, this provides at least two additional redundant actuators. These redundancies create non-unique solutions for controlling the aircraft, providing the ability to reconfigure in the case of failure. In addition to failure reconfiguration, additional actuators provide for the ability to optimize the control response in non-failure configurations.

Many studies on control allocation of multicopters have been conducted. Most focus on control reconfiguration and robustness in case of failure and are largely simulation-based such as [5, 6]. There have also been some flight studies in this area such as [7]. Fault tolerance is clearly an important issue, but at the same time, government, industry and academia have also been struggling to define the basic minimum flying qualities needed for these systems. In the limited literature focusing on the handling/flying qualities of multicopters, control allocation has not been considered as an important part of the equation. Control allocation has largely been focused on a pseudo-inverse solution employed where thrust is allocated equally to all rotors and the pitch and roll allocation are based on the distance of the arms from the center [8]. This is the minimum power solution for hover. However, it may be possible to use control allocation to modify the handling qualities of a vehicle with control redundancy, by taking advantage of the dynamic changes that occur when operating at high versus low rotational speed. Because of nonlinear relationships of rotor thrust, torque and power to rotor speed, a rotor operating at a higher rotational speed has faster dynamics but draws more power as compared to the same rotor operating at lower rotational speed, which will draw less power but result in slower dynamic response (e.g. a longer thrust time constant). Imagine the situation where roll response speed and precision were very important, and it might be possible to distribute higher rotational speed to the roll motors to achieve better rolling moment response. This will come with a power tradeoff and potentially degrade the response characteristics in other control axes. However, it may be worth this tradeoff in certain operational environments, such as navigating a narrow canyon.

In addition to evaluating the effect of control allocation on handling qualities of small multicopters, it is of interest to determine how these techniques

would translate to larger vehicles that would be appropriate for urban air mobility applications. There is increased interest in handling qualities of large multicopters, considering their role in advanced air mobility [9]. The study of handling/flying qualities for small scale multicopters has been shown to translate well to larger manned and unmanned multicopters (such as the H-47 Chinook), in [10]. Although it is unclear whether larger vehicles will by controlled in full by variable speed rotors, it is likely that at least in some configurations it will be used in combination with collective pitch and/or aerodynamic surfaces [11]. These large multicopters will be operated in a wide range of conditions, and will at least initially be piloted by humans, making handling qualities an area of key interest. Additionally, the same control system characteristics that make aircraft handle well in a range of conditions for manned operations also make them safer for unmanned operations, as shown by other unmanned aircraft that are based on manned frames, such as the Fire Scout [12].

This study will further extend on-going work in small and large multicopter handling qualities [1, 11] to investigate how control allocation of multicopters affects handling qualities. A key objective will be to study how this concept scales from smaller to larger vehicles. This is an important data point in the general handling qualities literature, where scaling techniques can save time and money in development of large multicopters, considering the reduced cost and risk of operating smaller vehicles.

This paper will first describe the small-scale test vehicle and then will show how the concept for multicopter control allocation works. The paper will then apply the concept to the small-scale test vehicle and perform system identification in flight to validate the changes in the dynamics of the system due to control allocation. Next, a control system optimization will be performed to take advantage of the control allocation. The concept will be flight tested to show handling qualities effects using autonomous mission task elements (MTEs) developed in Ref. [13]. Finally, the concept will be applied to a full scale (passenger) multicopter to explore scalability of the methods.

SMALL-SCALE TEST VEHICLE

The test vehicle used to perform initial evaluations of the concept of control allocation for handling qualities optimization is the UP Hexacopter, shown in Figure 1. The vehicle (UP Hexacopter) falls within the Group I UAS (<20 lb.). This custom hexacopter weighs 1.56 kg with a 4S battery and is 56 cm in diameter (hub-to-hub). The hexacopter was built using a DJI Flame-wheel F550 frame, six 930 kV motors, 30A electronic speed controllers and 10-inch diameter rotors. A Pixhawk Cube autopilot with open source ArduPilot software was used to control the aircraft [14]. In this research, a custom flight mode was developed using Simulink for the flight control system design and then implemented on the C++ based ArduPilot by using the Simulink® Coder functionality to generate C++ code of the control laws. The UP hexacopter also shares information with a ground control station (GCS) using a wireless 3DR 915MHz telemetry radio, using the mission planner software [15]. The ground control station, Mission Planner, was utilized to show real-time data on the UAV's position, upload commands, and set parameters. A motor kill switch and tethering system attached to the hexacopter were implemented to ensure safety.

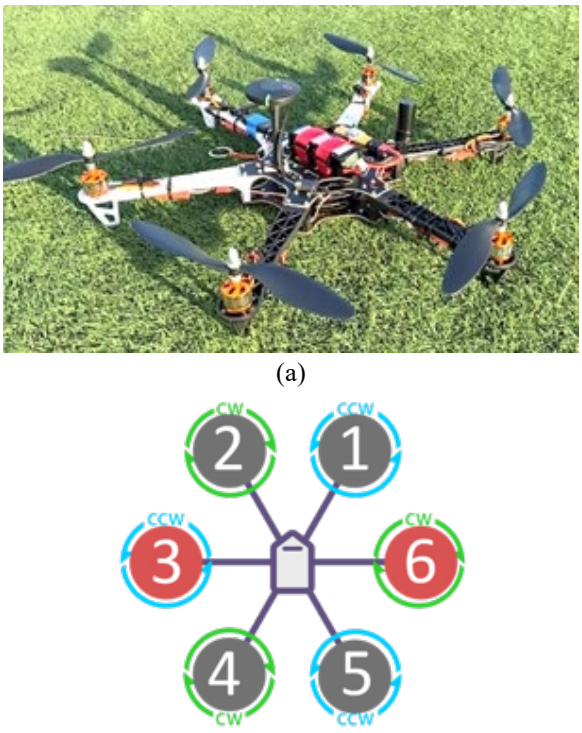

Figure 1. University of Portland hexacopter (a) flight configuration and (b) motor diagram.

Vehicles of this size are of practical use as a result of their size and maneuverability. Additionally, the dynamics of this size multicopters are scalable to larger configurations [10, 16], and therefore makes a safe and cost-effective test vehicle for control

allocation research. It is also helpful that this vehicle has a large power margin, and hovers at approximately 40% throttle, allowing for a range of control allocation configurations with less concern for saturation.

CONCEPT FOR VARIABLE SPEED CONTROL ALLOCATION

Typically, variable speed multicopter aircraft are trimmed with equal speed on each rotor. The force generated by each rotor can be modeled as shown, where the thrust T and torque Q of the ith rotor are related to the square of the rotor speed Ω:

$$T_i = \mu\Omega_i^2 \tag{1}$$

$$Q_i = \kappa\Omega_i^2 \tag{2}$$

However, using these models lacks multiple factors in analysis, and does not include the drag, side force, or pitching and rolling moments that occur during forward flight [3]. An important consideration of the dynamics with regards to flying qualities, particularly gust rejection, is that the control input, which drives the armature voltage of the electric motors V_a is proportional to rotational speed of the motor ω, not ω^2, which can be seen from the motor-rotor dynamics from [1, 4]. This can be seen from the motor-rotor dynamics from [1]:

$$L_A\frac{di_a}{dt} = -R_a i_a - K_e\omega + V_a \tag{3}$$

$$(I_r + Jr^2)\frac{d\omega}{dt} = K_m r i_a + \frac{\partial Q_A}{\partial\omega}\omega \tag{4}$$

Where the armature voltage, V_a is the input. An implication of this solution with regards to handling qualities is that the control input, which is the voltage or pulse width modulation input, is proportional to ω, not ω^2. Note that in this paper, all motors are assumed to be direct drive such that motor speed ω is equivalent to the rotor speed, Ω.

When considering the models used for control design and handling qualities analysis of the system, which are almost exclusively linear state-space models, the control inputs drive changes in the angular velocity, not the angular velocity squared. This is important because it indicates that the control effectiveness, as seen by the control system, is a function of the trim angular speed of the rotor. The linearized vertical acceleration control derivative (positive down) for each rotor can be determined:

$$\begin{aligned} Z_{\bar{x}_i} &= \frac{1}{m}\left(-\frac{\partial T}{\partial\bar{x}_i}\right)\Big|_{\bar{x}_{i_o}} \\ &= -\frac{1}{m}\left(\frac{\partial T}{\partial\Omega_i}\right)\Big|_{\omega_{i_o}}\left(\frac{\partial\Omega_i}{\partial\bar{x}_i}\right)\Big|_{\bar{x}_{i_o}} \end{aligned} \tag{5}$$

Where $\bar{x}_i$ is a normalized pulse width modulation (from 0 to 1) command on each individual motor. Using the simple propeller dynamics (where T is positive up):

$$\frac{\partial T}{\partial\Omega_i}\Big|_{\Omega_{i_o}} = 2\mu\Omega_{i_o} \tag{6}$$

And assuming a constant ratio of speed with normalized pulse width modulation (PWM) input, for small perturbations, and using the K_v rating of the (direct driven) motor, which provides the rated angular speed per volt applied. When using a direct drive system:

$$\frac{\partial\Omega_i}{\partial\bar{x}_i} = \frac{\omega_{max} - \omega_{min}}{\bar{x}_{i_{max}} - \bar{x}_{i_{min}}} = K_v V_{battery} \tag{7}$$

This shows that the linearized heave control derivative is a function of the trim speed of the rotor:

$$Z_{\bar{x}_i} = -\frac{2\mu K_v V_{battery}}{m}\Omega_{i_o} \tag{8}$$

As a result, the control derivative of each individual motor, $\frac{\partial T_i}{\partial\bar{x}_i}$, or the thrust response to control perturbation, $\bar{x}_i$, is a strong function of the trim angular speed Ω_{io}. Although the control mechanism is different, this is consistent with the effects of variable speed rotors observed by Chen in full-scale helicopters, where the lower the rotor speed, the more sluggish handling qualities were reported in Ref. [17] as indicated by the significantly reduced vertical damping.

This clearly has important implications on handling qualities in terms of the selection of the rotor size, number of rotors and associated trim rotor speed for multicopters. For example, when all the rotors are the same size and are trimmed at the same speed, then

$$\Omega_{i_o} = \sqrt{\frac{mg/n}{\mu}} \tag{9}$$

This indicates that

$$Z_{\bar{x}_i} = -2\left(\frac{g\mu}{mn}\right)^{0.5} K_v V_{battery} \tag{10}$$

And the basic thrust derivative, in units of force per normalized input is

$$T_{\bar{x}_i} = -mZ_{x_i} = 2\left(\frac{mg\mu}{n}\right)^{0.5} K_v V_{battery} \tag{11}$$

This result is interesting because it shows that as mass increases and the number of rotors increases, the effective control derivative of each rotor is proportional with $\sqrt{m/n}$. So, for example, comparing a quadcopter, hexacopter, and octocopter from [18], which all use the same rotor size, motors, and batteries:

$$m_{quad} = 6.1 \text{ kg} \tag{12}$$

$$m_{hexa} = 7.1 \text{ kg} \tag{13}$$

$$m_{octo} = 8.2 \text{ kg} \tag{14}$$

This indicates that for these aircraft, the basic thrust control derivative per motor will increase with decreasing number of rotors, because the mass does not scale proportionally with the number of motors. Because the quadcopter motors must operate at a higher trim speed than the octocopter or hexacopter, due to the proportionally higher mass per rotor, the quadcopter is predicted to have 22% higher thrust output per unit input per motor than the octocopter, and 13% more than the hexacopter:

$$\frac{T_{\bar{x}_i quad}}{T_{\bar{x}_i octo}} = \sqrt{\left(\frac{m_{quad}}{4}\right)\left(\frac{8}{m_{octa}}\right)} = 1.22 \tag{15}$$

$$\frac{T_{\bar{x}_i quad}}{T_{\bar{x}_i hexa}} = \sqrt{\left(\frac{m_{quad}}{4}\right)\left(\frac{6}{m_{hexa}}\right)} = 1.13 \tag{16}$$

This is consistent with Ref. [18], where this ratio was approximately $\frac{T_{\bar{x}_i quad}}{T_{\bar{x}_i octo}} = 1.3$ and $\frac{T_{\bar{x}_i quad}}{T_{\bar{x}_i hexa}} = 1.04$ from the flight identified derivatives. Although the predictions of Eqs. (15-16) are imperfect, they are within $\pm 12\%$, providing a rough estimate. Although the trends are correct, in reality, the thrust coefficient μ is affected by inflow, which varies with rotor speed and interference effects. Combined, these approximations are likely the source of the additional discrepancy in this simple theory and the system identified results.

That the trim rotor speed effects the control responsiveness implies that it cannot be ignored as an important element of the control system design. In [18], significant differences in disturbance rejection were found for the varying configurations. In part, this was due to this loss of thrust control derivative as the number of motors increased. There is also an important associated reduction of pitch and rolling moment control. It was also seen that the systems with more rotors operating at lower trim speed had lower effective pitch damping M_q (and roll damping L_p due to symmetry).

Off-Nominal Trim RPM

The dependency of stability and control derivatives on the trim rotational speed of the rotors suggests that for a given configuration the handling qualities could be modified by trimming some pairs of motors at higher RPM and some pairs of motors at lower RPM. For example, in Figure 1, rotor pair 3-6 could be trimmed at higher RPM, while rotor pairs 1-2 and 4-5 could be trimmed at lower RPM, while still providing the same trim thrust to balance weight. Although this will cause the power usage to be non-minimum, this increased control allocation arrangement to the rolling motors could improve handling qualities in the roll axis by increasing roll control effectiveness and roll damping. The power tradeoff and lower pitch control effectiveness may be acceptable in conditions where roll axis is critical to flight safety, like operations in turbulent narrow urban canyons where a tight lateral track must be maintained. A similar tradeoff could be made in pitch for temporary operations in which pitch gust rejection is critical by increasing the RPM on the 1-2 and 4-5 motors and reducing RPM on the 3-6 motor pair. This could aide precision landing in gusty conditions, such as on a rooftop or heliport, where pitch disturbance rejection is critical to complete a landing flare. This paper studies the effects of handling qualities when trimming in these alternate off-nominal configurations and evaluates the tradeoff between handling qualities and power usage in these off-nominal control allocation configurations.

MODEL PREDICTION OF CONTROL ALLOCATION EFFECTS ON FLIGHT DYNAMICS

In this section, the mixing configurations of interest are introduced, and then, the effect that the mixing has on the trim speed and associated thrust derivatives of each motor will be explored.

Nominal Mixer

The nominal mixer in the ArduPilot [14] control system used for the UP hexacopter that was considered in this work can be approximated by:

$$\begin{bmatrix} PWM_1 \\ PWM_2 \\ PWM_3 \\ PWM_4 \\ PWM_5 \\ PWM_6 \end{bmatrix} = K_{PWM} \begin{bmatrix} 1 & 0.25 & -0.5 & 0.5 \\ 1 & -0.25 & -0.5 & -0.5 \\ 1 & -0.25 & 0 & 0.5 \\ 1 & -0.25 & 0.5 & -0.5 \\ 1 & 0.25 & 0.5 & 0.5 \\ 1 & 0.25 & 0 & -0.5 \end{bmatrix}_{nominal} \begin{bmatrix} \delta_{thr} \\ \delta_{lat} \\ \delta_{lon} \\ \delta_{yaw} \end{bmatrix} \quad (17)$$

Where K_{PWM} is a scale factor converting to units of pulse width modulation. The first column indicates how the throttle input is mapped into the pulse width modulation command for each motor. By setting all elements in this column to one, this ensures that the trim thrust is distributed equally among the rotors at hover where there are no significant aerodynamic pitch, roll or yaw moments. Note that the inputs and outputs of the mixer in Ardupilot are not perturbation values but carry the full solution including trim.

Off-Nominal Mixers

A simple way to put the multicopter into the off-nominal trim condition described earlier, where some pairs of motors have increased speed and others have lower speed, is by modifying the throttle mapping in the mixer. The allocation used herein only manipulates the throttle mapping terms. The heave mixing terms are designed to add up to n, or six in the case of the hexacopter, to limit scaling effects in the heave axis. For the same reason, the longitudinal, lateral and yaw mixing terms remain unchanged in the off-nominal configuration.

$$\begin{bmatrix} PWM_1 \\ PWM_2 \\ PWM_3 \\ PWM_4 \\ PWM_5 \\ PWM_6 \end{bmatrix} = K_{PWM} \begin{bmatrix} 0.75 & 0.25 & -0.5 & 0.5 \\ 0.75 & -0.25 & -0.5 & -0.5 \\ 1.5 & -0.25 & 0 & 0.5 \\ 0.75 & -0.25 & 0.5 & -0.5 \\ 0.75 & 0.25 & 0.5 & 0.5 \\ 1.5 & 0.25 & 0 & -0.5 \end{bmatrix}_{3-6\ High} \begin{bmatrix} \delta_{thr} \\ \delta_{lat} \\ \delta_{lon} \\ \delta_{yaw} \end{bmatrix} \quad (18)$$

$$\begin{bmatrix} PWM_1 \\ PWM_2 \\ PWM_3 \\ PWM_4 \\ PWM_5 \\ PWM_6 \end{bmatrix} = K_{PWM} \begin{bmatrix} 1.25 & 0.25 & -0.5 & 0.5 \\ 1.25 & -0.25 & -0.5 & -0.5 \\ 0.5 & -0.25 & 0 & 0.5 \\ 1.25 & -0.25 & 0.5 & -0.5 \\ 1.25 & 0.25 & 0.5 & 0.5 \\ 0.5 & 0.25 & 0 & -0.5 \end{bmatrix}_{3-6\ Low} \begin{bmatrix} \delta_{thr} \\ \delta_{lat} \\ \delta_{lon} \\ \delta_{yaw} \end{bmatrix} \quad (19)$$

Throughout the paper the three control mixing schemes presented in Eqs. (17-19) are referred to as: the nominal configuration (Eq. 17), off-nominal 3-6 High configuration (Eq. 18) and off-nominal 3-6 Low configuration (Eq. 19).

Evaluation of Off-Nominal Mixing with RMAC

Flight-accurate state-space models of the vehicle with nominal mixing have been developed via frequency domain system identification in Refs. [16, 19], at hover and 5 m/s flight conditions, using the CIFER® software [20]. However, these linear models are not capable of predicting trim or extrapolating the nonlinear effects of off-nominal trim RPM due to off-nominal mixing. To evaluate these nonlinear effects, the Rensselaer Multicopter Analysis Code (RMAC) was used to determine trim conditions for the off-nominal mixers and provide linearized models at these conditions. RMAC is a nonlinear blade-element model and comprehensive analysis tool [21]. RMAC has already been extensively validated against the UP Hexacopter in [19]. Although it is not as accurate as a system identification model, RMAC captures the on-axis angular rate responses reasonably well at frequencies in the range of the expected broken loop crossover frequency (~ 10 – 20 rad/s) and thus is acceptable for flight control design purposes.

Using the nominal and off-nominal mixers presented in Eqs. (17-19) the trim speed in RPM and thrust derivatives (in units of μN/RPM) results are calculated and presented in Figure 2. As shown in the Figure, the Nominal Mixer has the same trim rotor speed across all configurations (~4500 RPM). Additionally, the 3-6 Low configuration has lower trim speed on the rolling motors (3, 6) and higher trim speed than nominal on the pitching motors (1, 2, 4, 5). In Figure 2a the 3-6 High Mixer configuration shows higher trim RPM on the rolling motors (3, 6), and lower trim RPM on the other motors (1, 2, 4, 5). Figure 2b shows that the

linear thrust control derivative for each motor, T_{RPM}, which indicates the amount of thrust (in μN) generated per ΔRPM around the trim condition. The linear thrust derivative T_{RPM} varies approximately linearly with the trim RPM, as expected.

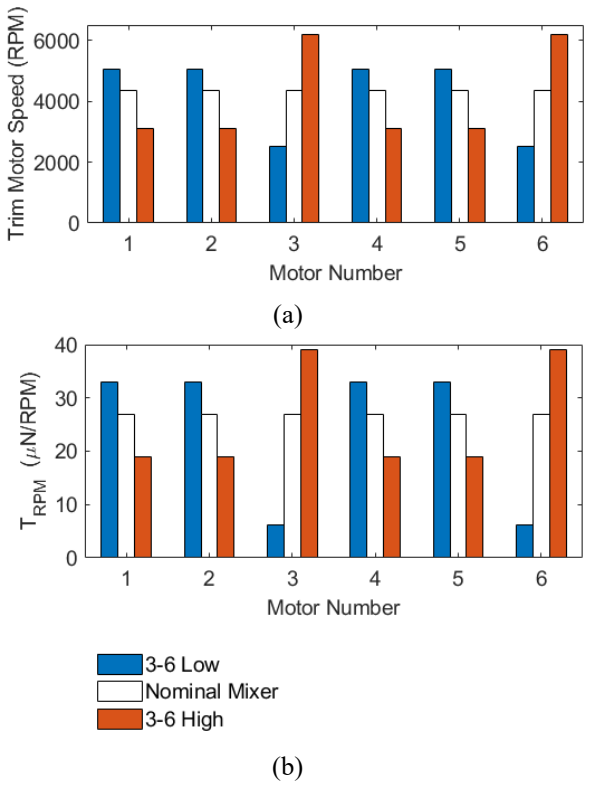

Figure 2. Trim rotor speed and resulting thrust control derivatives per motor from RMAC.

The changes in the derivatives from the individual motors are reflected in the stability and control derivatives of the aircraft when taken as a whole. This can be seen in Figure 3a, where for example, the 3-6 High mixing results in an increase in the throttle derivative Z_{thr} relative to the nominal mixer, but a decrease in heave damping Z_w, as well as yaw control N_{yaw} and yaw damping N_r derivative terms. Additionally, in Figure 3b, the 3-6 High mixing increases the roll control L_{lat} and roll damping L_p derivatives, while resulting in a decrease of the pitch damping M_q and pitch control M_{lon} terms. This is expected because of the higher RPM on the rolling motors (3,6) in this configuration. Conversely, for the 3-6 Low configuration, lower RPM on the rolling motors decreases the roll damping L_p and roll control L_{lat} derivatives, and higher RPM increases the pitch damping M_q and pitch control M_{lon} terms. The speed damping terms L_v and M_u are decreased somewhat in both off-nominal mixing configurations.

Another tradeoff to the off-nominal mixers is shown in Table 1. These configurations also require increased power consumption because the minimum power solution is found when the identical motors carry an evenly dispersed load. Although we gain roll damping and control effectiveness in the 3-6 High configuration, the tradeoff is an increased power usage of about of about 17%. Due to this fact, these off-nominal control allocation mixers should only be applied in circumstances where high precision is required in a certain axis, such as a situation where heightened roll control is needed; for example, in high crosswinds or narrow canyons.

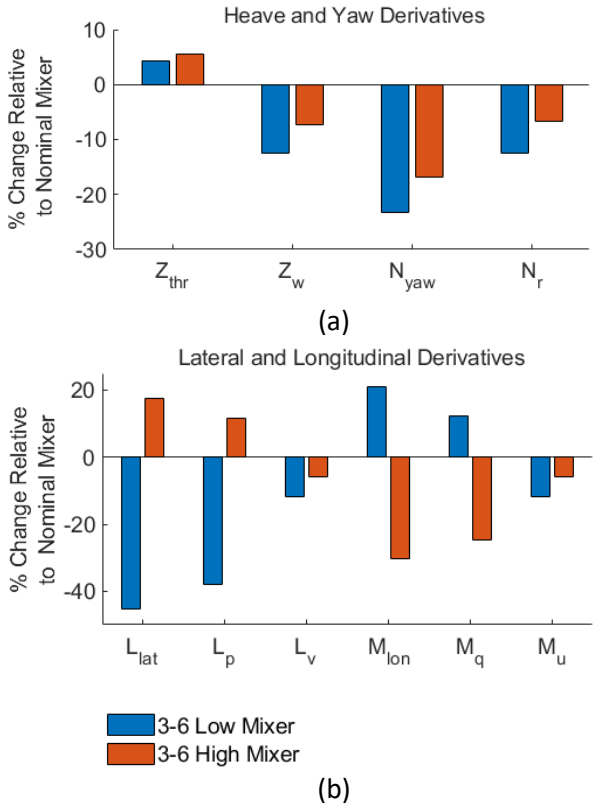

Figure 3. Stability and control derivatives for the total aircraft from RMAC.

Table 1. Trim power, predicted by RMAC.

Mixer	***Trim Power (Watts)***
Nominal	113
3-6 High	133
3-6 Low	127

FLIGHT VALIDATION OF FLIGHT DYNAMICS WITH OFF-NOMINAL MIXING

To validate the RMAC models, trim data and frequency sweeps were conducted with the nominal mixer, and the two off-nominal mixers presented in Eqs. (18) and (19). For the off-nominal mixer validation, the off-nominal mixers were programmed into Ardupilot by programming a custom throttle scale factor in the AP_motors library.

Trim Validation at Hover

To validate trim rotor speed in flight, the pulse width modulation (PWM) commands to the motors were measured in a steady hover. These commands were averaged over approximately ten seconds, and small imbalances in the motor trims were averaged (even in the nominal case all six motors have slightly different mean trim values over the ten second window). There is no direct measurement of motor speed on the UP Hexacopter so the PWM commands were converted to estimated speed output values. The conversion factor from command PWM to motor speed was determined via testing with a contact tachometer. Although this is not as accurate as direct measurement of rotational speed in flight, this method provides a reasonable estimate of the flight rotor/motor speed for validation purposes.

Results of the trim validation are shown in Table 2. The RMAC prediction of the trim speed is reasonably good, with errors not exceeding 16%, as compared to flight data. We can see that the mixer is correctly implemented in the Hexacopter and that the trim values follow the expected trends from RMAC that were shown in Figure 2.

Table 2. Trim rotor speed, RMAC predicted and from flight.

	Trim Rotor Speed (RPM)					
Motor Number	**1**	**2**	**3**	**4**	**5**	**6**
Nominal Mixer RMAC	4368	4368	4368	4368	4368	4368
Nominal Mixer Flight	4422	4422	4422	4422	4422	4422
% Error	-1.2%	-1.2%	-1.2%	-1.2%	-1.2%	-1.2%
3-6 High	3085	3085	6170	3085	3085	6170
3-6 High Flight	3450	3450	5305	3450	3450	5305
% Error	-11%	-11%	16%	-11%	-11%	16%
3-6 Low	5032	5032	2511	5032	5032	2511
3-6 Low Flight	4781	4781	3005	4781	4731	3005
% Error	5.3%	5.3 %	-16%	5.3%	5.3%	-16%

Frequency Response Validation at Hover

To perform validation of the effects of off-nominal mixing, frequency domain system identification was performed with the off-nominal mixers in place. Frequency sweeps were collected in flight, using a frequency range of 1 rad/s to 50 rad/s, in the built-in system identification mode available in ArduPilot. The frequency responses were identified using the CIFER® software tool [20]. Figure 4 and Figure 5 provide pitch and roll hover response validation of the RMAC model as compared to the flight data for the nominal and off-nominal mixers. It should be noted that coherence below 1 rad/s and above 50 rad/s is low, indicating that the frequency response is less accurate, as expected due to the frequency range of the frequency sweep. In both pitch and roll, for the nominal mixer, RMAC accurately predicts the higher frequency dynamics (> 6 rad/s) although with slightly reduced gain and has a larger mismatch in the lower frequency unstable phugoid-like mode (< 3 rad/s). There is acceptable accuracy near the expected crossover frequency (12-15 rad/s). Thus, the model is acceptable to use for flight control design as discussed in [19]. The RMAC model for the 3-6 High mixer has similar trends, where the phugoid mode damping is too low as compared to flight data, resulting in a magnitude mismatch at frequencies between 1 – 5 rad/s. The high frequency gain (> 6 rad/s) is also underpredicted with the off-nominal mixer. However, the trends between the off-nominal mixer and the nominal mixer are correctly predicted by RMAC. For the pitch response, shown in Figure 4, RMAC predicts a decrease in magnitude of about a 18% relative to the nominal mixer for frequencies greater than 6 rad/s, and is consistent in the flight data as seen by the ~1.5 dB

loss of magnitude relative to the nominal mixer flight data. For the roll response, shown in Figure 5, RMAC predicts an increase in magnitude and phase from 3 rad/s to 20 rad/s. The flight data also sees a similar trend with increased magnitude and phase relative to the nominal flight data.

The yaw response shown in Figure 6 is not as well predicted by RMAC. The flight data has some unexpected phase loss and loss of magnitude at low and high frequency. It is clear in flight that the off-nominal mixer influences the yaw response, reducing magnitude at low and high frequency. The phasing differences could be due to the very low RPM that is on four of the motors (motors 1,2,4,5), creating a hysteresis-like response in the torque response (which generates a constant phase shift downward) for those motors. For brevity, the heave response is not shown because very little change in the heave response was predicted or seen in the flight data. It should be noted that frequency sweeps for the 3-6 Low mixers were also conducted and the flight frequency responses were evaluated against the RMAC predictions. The flight responses for the 3-6 Low mixer proved to have similar trends as expected from RMAC, and similar discrepancies compared to the flight data as seen in Figure 4 - Figure 6, but are not shown for brevity.

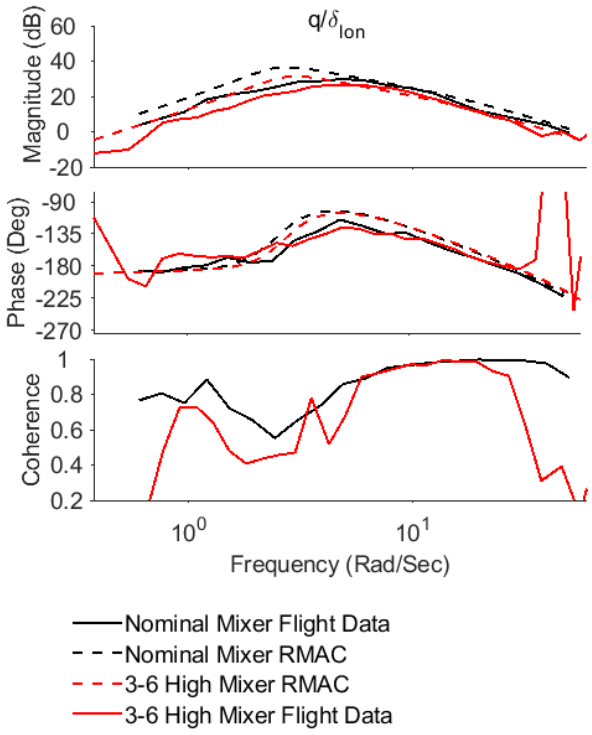

Figure 4. Pitch rate comparison of RMAC model and flight data, with nominal and 3-6 High mixers.

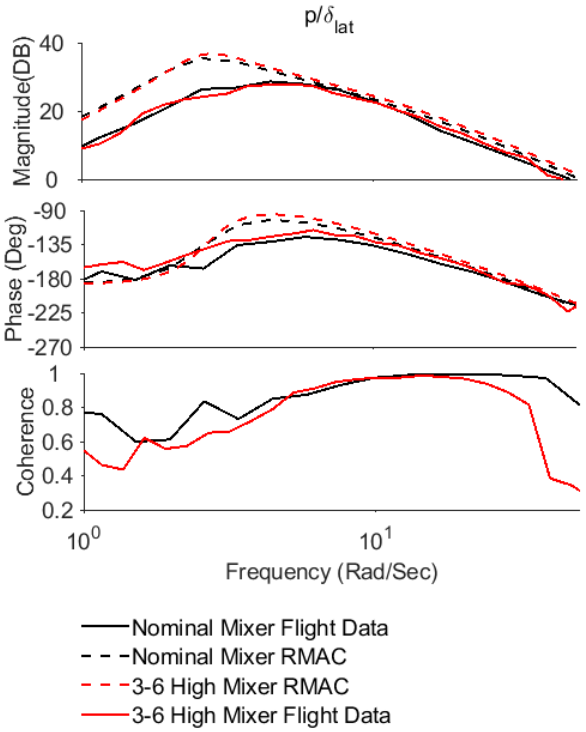

Figure 5. Roll rate comparison of RMAC model and flight data, with nominal and 3-6 High mixers.

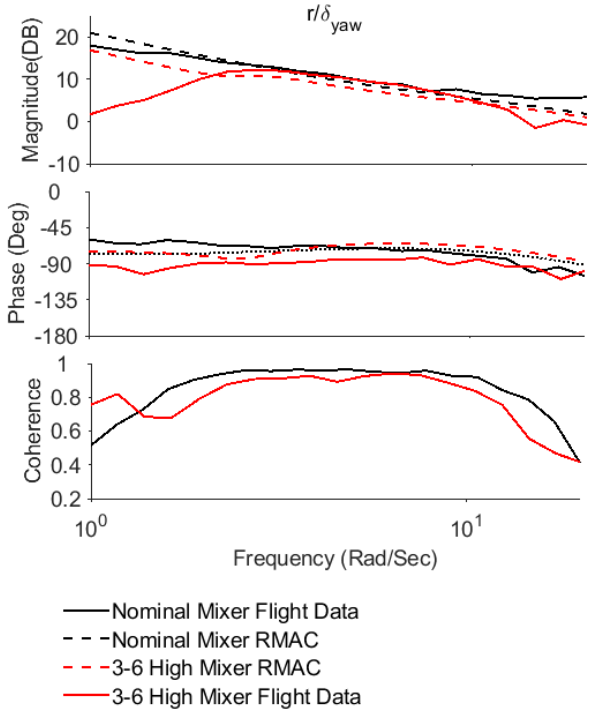

Figure 6. Yaw rate comparison of RMAC model and flight data, with nominal and 3-6 High mixers.

As predicted by RMAC, the modes of the hexacopter change depending on the control allocation configuration, as confirmed by Table 3. In Table 3, the RMAC and flight identified model are shown. The high costs seen in the RMAC model are due to the poor prediction of the phugoid mode, as discussed in [19]. The flight identified model was determined via transfer function fitting. The transfer function fit was performed in the NAVFIT tool in CIFER® [20], where a weighted least-squares fit of magnitude and phase is minimized. A third-order transfer function was fit to capture the hovering cubic. For the 3-6 High configuration, the roll mode increases in frequency as compared to the nominal configuration as predicted by RMAC and seen in the flight data. This is expected due to the increased thrust and responsiveness associated with the roll motors and reduced thrust and responsiveness associated with the pitch motors. In an alternate configuration, 3-6 Low, which de-weights the roll motors and trims with higher RPM on the pitch motors, the opposite effect is found.

Table 3. Transfer function fit to identified flight data in the roll axis.

	Roll Mode λ_{roll} ***(rad/s)***	***Roll Control*** $L_{\delta_{roll}}$	***Phugoid Mode*** ζ, ω_n	***Cost, J*** p/δ_{lat} ***(1.5 – 25 rad/s)***
3-6 High RMAC	-4.4	205	$\zeta = -.292,\ \omega_n = 2.64$ rad/s	600
3-6 High Flight	-4.2	160	$\zeta = -.499,\ \omega_n = 3.36$ rad/s	38
Nominal RMAC	-4.3	154	$\zeta = -.32,\ \omega_n = 2.75$ rad/s	524
Nominal Flight	-4.0	120	$\zeta = -.53,\ \omega_n = 3.5$ rad/s	31
3 6 Low RMAC	-3.69	84.8	$\zeta = -.37,\ \omega_n = 2.78$ rad/s	279
3-6 Low RMAC Flight	-3.67	62.3	$\zeta = -.55,\ \omega_n = 3.18$ rad/s	68

CONDUIT® DESIGN MARGIN OPTIMIZATION

With the RMAC model trends for the roll mode and roll control derivatives validated in flight for off-nominal configurations based on flight identified frequency responses, control system optimizations with the off-nominal mixers in place were completed using the CONDUIT® software (Ref. [22]). Although the RMAC model is known to not provide an accurate prediction for the phugoid mode, this is not important for flight control because it is well below the crossover frequency. The goal of these optimizations was to determine closed-loop performance improvements and trade-offs that result from the off-nominal mixing in certain axes. In short, the goal was to answer the question: Can these off-nominal mixing matrices result in improved closed loop control system performance in certain control axes when optimized to exploit the changes in the flight dynamics?

The control system was optimized against the same set of specifications used in the control systems designs used for Level 1 handling qualities evaluations in Ref. [10]. Many of the specifications were Froude scaled from ADS-33E-PRF, which was found to provide satisfactory handling qualities in flight. The set of optimization specifications is shown by Table 4.

Inner Loop Attitude Control System

A design margin optimization (DMO) was performed on each of the three mixing models extracted from RMAC for the attitude command controller. The control system, which is described fully in [10] and shown in Figure 7 was re-optimized for the three RMAC models, using design margin optimization. The design margin optimization was applied to the disturbance rejection bandwidth and crossover frequency specifications, as recommended in [22]. This optimized a series of control systems with incrementally increasing required disturbance rejection bandwidth (DRB), above the Froude scaled Level 1 boundary. A higher design margin would warrant a faster disturbance rejection response, and better tracking of commands in the case of turbulence and uncertainty.

Table 4. Design specifications for pitch/roll axes.

Design Specification	***Constraint Type***	***Froude Scaled?***	***Inner Loop Level 1/2 Boundary (Pitch/Roll Attitude)***	***Outer Loop Level 1/2 Boundary (Longitudinal/Lateral)***	***Design Margin Applied***
Eigenvalues	Hard	No	$\lambda \leq 0$	$\lambda \leq 0$	No
Stability Margins	Hard	No	GM ≥ 6 dB, PM ≥ 45 deg (inner loop)	GM ≥ 6 dB, PM ≥ 35 deg (outer loop)	No
Minimum Crossover Frequency	Soft	Level 1/2 Boundary	$\omega_c \geq 12.5$ rad/s (at actuator)	$\omega_c \geq 12.5$ rad/s (at actuator)	Yes
Disturbance Rejection Bandwidth	Soft	Level 1/2 Boundary	$\omega_{DRB_{\phi,\theta}} \geq 4.19$ rad/s	$\omega_{DRB_{X,Y}} \geq 0.79$ rad/s $\omega_{DRB_{u,v}} \geq 2.51$ rad/s	Yes
Disturbance Rejection Peak	Soft	No	DRP ≤ 5 dB	DRP ≤ 5 dB	No
Damping Ratio	Soft	Frequency Range	$\zeta \geq 0.35$ (modes ≤ ω_c)	$\zeta \geq 0.3$ (modes ≤ ω_c)	No
Model Following	Soft	Frequency Range	$J_{mf} \leq 50$	n/a	No
Actuator RMS	Summed Objective	No	Minimize	Minimize	No
Crossover Frequency	Summed Objective	No	Minimize	Minimize	No

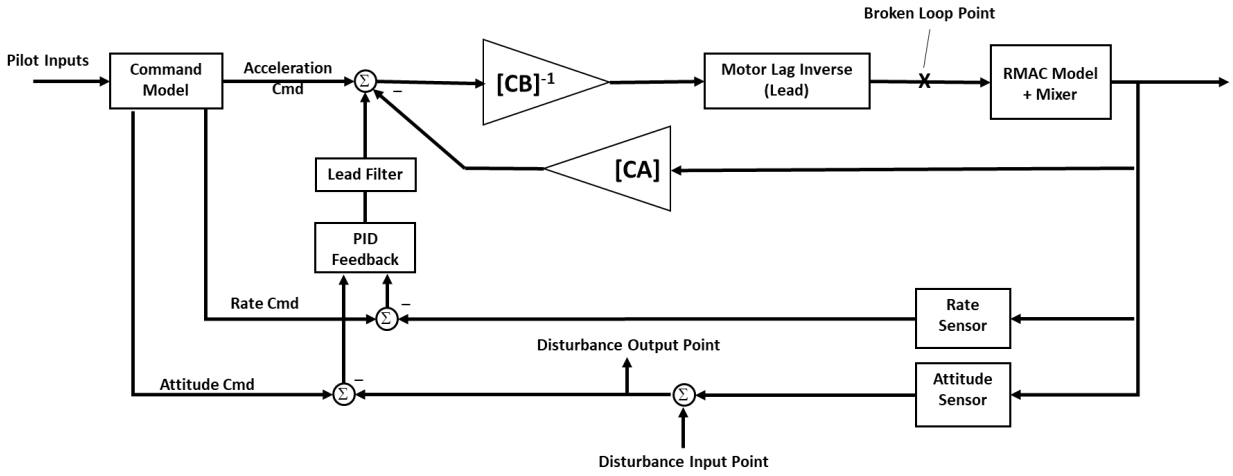

Figure 7. Attitude command with model following dynamic inversion architecture [10].

Table 5. Optimized maximum disturbance rejection characteristics for the attitude command system.

	DRB *(rad/s)* *(Disturbance Rejection Bandwidth)*			***DRP*** *(dB)* *(Disturbance Rejection Peak)*		
	Nominal	**3-6 Low**	**3-6 High**	**Nominal**	**3-6 Low**	**3-6 High**
Roll	5.44	5.29	5.65	3.90	3.85	3.77
Pitch	5.44	5.96	5.65	4.04	3.98	3.88
Yaw	4.23	4.04	4.39	3.12	3.18	3.00

Shown in Table 5 are the maximum achievable DRB for each axis for the different mixer configurations. DRB represents a system's ability to reject disturbances, so, the higher the DRB value, the better a system rejects disturbances. For the Nominal mixer, we can see that the roll and pitch DRB values are equal at 5.44 rad/s due to the symmetry of the configuration. In the off-nominal mixing, asymmetry between pitch and roll response dynamics are introduced, resulting in different maximum values between the pitch and roll axes. The 3-6 Low exhibits a higher DRB in the pitching axis (as the pitching motors have increased allocation), and lower DRB in the rolling axis. 3-6 High on the other hand exhibits a higher DRB in both the roll and pitch axes; however, it ultimately has highest DRB in the roll axis at 5.65 rad/s. The 3-6 Low configuration has lower DRB in the yaw axis than nominal, while 3-6 High has higher DRB than nominal.

Table 5 also presents the disturbance rejections peaks (DRP's) to express the amount of overshoot a system has during a disturbance rejection. In this case, the preferable response is a lower DRP value, as this means there is lower overshoot. Compared the nominal case, 3-6 Low has lower DRP in all axes besides the yawing axis. 3-6 High also has lower DRP than the nominal case.

Overall, the cases designed with the off-nominal mixers have better DRB in the expected axes. This is demonstrated with 3-6 Low, where it has higher DRB in the pitch axis but lower in the roll axis. The DRP results show that custom mixers should reduce overshoot compared with the nominal mixer, with an exception for the 3-6 Low mixer in the yawing axis.

Step plots for the time response to attitude disturbance in each axis are shown in Figure 8. The roll attitude disturbance response (Figure 8a) shows 3-6 High with the fastest response overall but it also has more overshoot than the nominal mixer. 3-6 Low in the rolling axis has the slowest response with most overshoot as the rolling motors have lower allocation in the roll axis. As expected, in the pitch axis shown in Figure 8b, 3-6 Low configuration performs the fastest disturbance rejection. It is also shown that while the response speed is faster in the pitching axis for 3-6 Low, it has a higher overshoot than the nominal mixer. Where 3-6 Low sacrifices roll performance for better pitch performance, 3-6 High sacrifices pitch performance for better roll performance.

In the yaw axis, shown in Figure 8c, little difference is seen between the nominal mixer and 3-6 High. 3-6 Low, however, has the slowest response with the least overshoot. This may be due to the four motors (1,2,4,5) at higher trim rotor speed associated with lower torque.

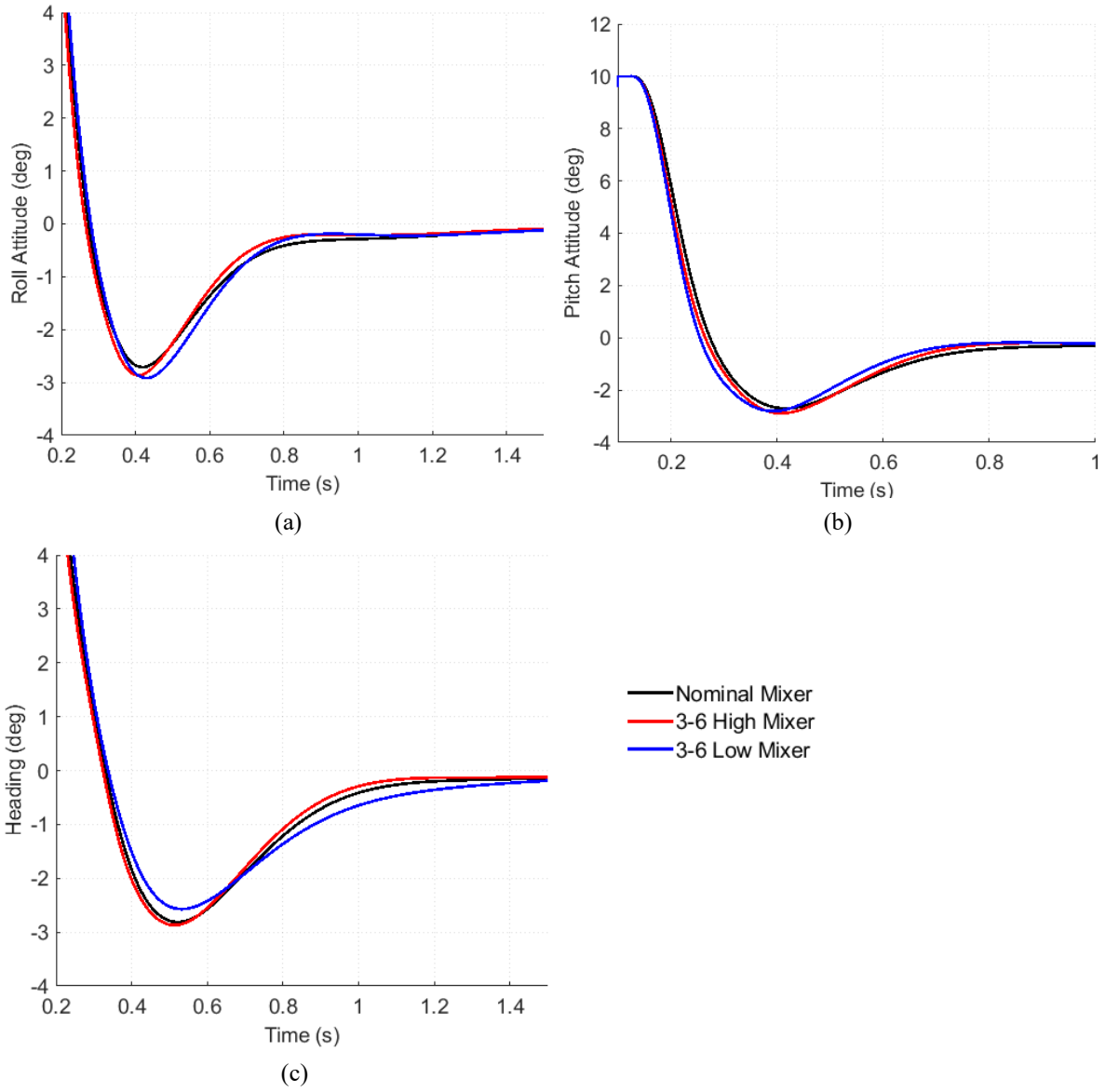

Figure 8. Simulated step response plots for attitude disturbance rejection in (a) roll, (b) pitch, and (c) yaw axes.

Outer Loop Position and Velocity Control

An outer loop that enables trajectory following is implemented as shown in Figure 9. This control system is fully discussed in Ref. [10]. The outer loops were optimized, using CONDUIT®, around the maximum disturbance rejection bandwidth optimized inner-loop gains for each of the three mixing configurations. The outer loop design was optimized just to the Level 1 requirements, without any design margin. This allows us to focus the results on the effect of the inner loop optimization and how that affects the outer loop system.

The results of the optimization are shown in Table 6 and Table 7. For the velocity disturbance rejection bandwidth (Table 6), the maximum lateral velocity DRB is found in the 3-6 High mixer, whereas the lowest lateral DRB is present in the 3-6 Low mixer configuration. The 3-6 Low mixer has lower DRP than the other configurations for the longitudinal velocity response, although the DRB is similar to the other configurations. The outer loop position DRB in Table 7 has similar performance for all three systems, which were all optimized to the same Level 1 requirement. However, the DRP value for the lateral axis is notably lower (better) for the 3-6 High mixer, and the DRP for the longitudinal axis is lowest for the 3-6 Low axis, following expected trends.

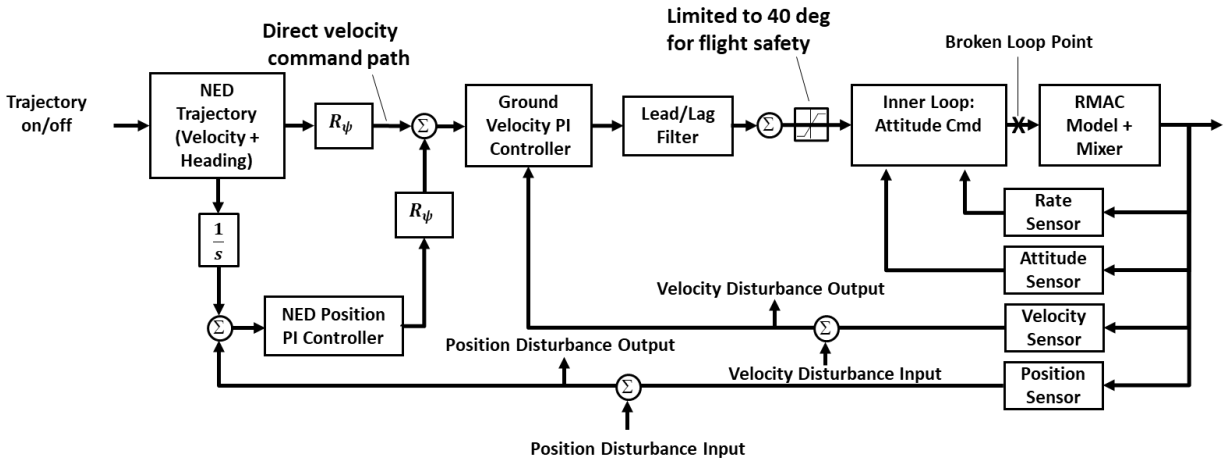

Figure 9. Outer loop control architecture.

Table 6. Optimized disturbance rejection characteristics for the velocity control loop.

	***DRB** (rad/s)*			***DRP** (dB)*		
	Nominal	**3-6 Low**	**3-6 High**	**Nominal**	**3-6 Low**	**3-6 High**
Longitudinal	3.5	3.3	3.0	4.5	3.8	5.2
Lateral	3.5	2.5	3.8	4.5	3.5	5.3
Altitude	5.0	5.0	5.0	4	3.4	3.5

Table 7. Optimized disturbance rejection characteristics for the position control loop.

	***DRB** (rad/s)*			***DRP** (dB)*		
	Nominal	**3-6 Low**	**3-6 High**	**Nominal**	**3-6 Low**	**3-6 High**
Longitudinal	0.80	0.81	0.79	2.3	2	2.2
Lateral	0.80	0.79	0.81	2.3	2.5	1.9
Altitude	0.90	0.90	0.90	0.32	0.4	0.46

An automated, Froude-scaled ADS-33E-PRF pirouette maneuver, as described in Ref. [13], was used to evaluate the performance of the outer loop control system in closed loop simulation with position, velocity and attitude controllers active. In prior flight tests, the pirouette has shown to have the closest simulation performance to flight because it excites pitch, roll and yaw simultaneously. The trajectory errors in the longitudinal and lateral axes are shown in Table 8 and a plot of the trajectory is shown in Figure 10. The largest errors in the trajectory can be seen in the 3-6 Low configuration, which is largely due to errors in the lateral tracking combined with lower heading tracking. The 3-6 High configuration, on the other hand, had improved lateral and heading tracking. In simulation, the 3-6 High configuration has about 18% improvement in the lateral tracking error, which is significant.

Table 8. Tracking errors for scaled pirouette MTE.

	Max Lateral Error (cm)	***Max Longitudinal Error (cm)***
Nominal	11	5.1
3-6 High	9	4.6
3-6 Low	18	5.4

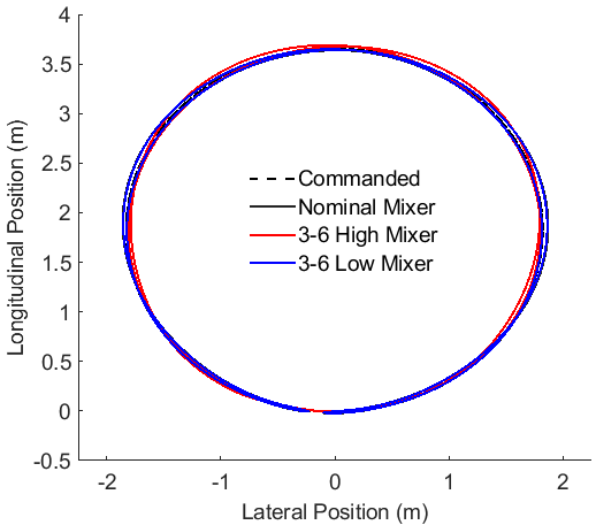

Figure 10. Scaled pirouette MTE from simulation.

FLIGHT TESTING FOR HANDLING QUALITIES

To evaluate the handling qualities on the actual flight vehicle, a scaled depart-abort maneuver was flown with the University of Portland Hexacopter. At least three runs were completed for each configuration. The depart-abort maneuver was scaled and evaluated using the framework developed by University of Portland and US Army DEVCOM as described in [13]. The depart-abort maneuver was selected to demonstrate the differences between the mixing configurations because a tight lateral trajectory is required during the maneuver, which was expected to highlight improvements of the 3-6 High mixing configuration.

Example data for one run for each of the three mixers is shown by Figure 11. As shown in the Figure, the 3-6 High mixing has the lowest lateral deviation from the desired forward path during the depart-abort maneuver. This can be seen in the position, as well as the velocity data shown in Figure 12. Additionally, the mean and standard deviation from three runs are shown in Figure 13, indicating that this trend was found throughout the three cases. Note that a Level 1 requirement of 0.4 m (1.35 ft) is recommended for the hexacopter scale in the proposed UAS handling qualities framework of Ref. [13], as reflected by the hashed line on the figure. The nominal mixing configuration shown was optimized using the flight identified model, because the optimization data using the RMAC model did not perform as well as the flight identified optimized control gains. The off-nominal configurations used corrections to the optimization model that helped it better approximate the flight data, although this was imperfect. Still, as shown in Figure 13, an improvement of approximately 15% for the lateral motion of the vehicle was achieved. This is a notable improvement, especially considering the imperfect model used in the optimization of the control system. The 3-6 Low configuration has significantly more error in the lateral motion, as expected due to the low RPM on the roll motors. It should be noted that the 3-6 High mixing configuration qualitatively flew well, but that the 3-6 Low mixing configuration was very difficult to fly. The 3-6 Low performance was jerky and near saturation in yaw. This qualitive assessment is hard to see that from the data plots, but obvious as an observer.

Although all the cases met the time requirement for maneuver completion, there were differences in the longitudinal trajectory tracking that are worth mentioning. As shown by Figure 12, the longitudinal velocity tracking for the 3-6 Low configuration is slightly improved with less lag initially as compared to the nominal mixing. This is surprising considering the jerky longitudinal motion observed for this case, where the jerkiness is likely due to the yaw axis operating near saturation. In Figure 14, the mean and standard deviation longitudinal position error (relative to the commanded trajectory) is shown. The figure indicates that the nominal mixer and the 3-6 Low mixer had similar average performance, although the nominal case was more variable with one case having a maximum longitudinal tracking error of 0.9 m. The 3-6 High configuration had degraded performance in the longitudinal tracking, which is consistent with the trades-off notated throughout this paper.

Overall, a 15% improvement in the lateral tracking was seen for the 3-6 High configuration, which represents a substantial improvement and is near the percent improvement predicted by simulation (18%). However, the longitudinal axis was not as fast to respond as seen in the lagged longitudinal velocity response of Figure 12. This is an expected tradeoff of this configuration because the pitching motors are operating at lower speed than the roll motors.

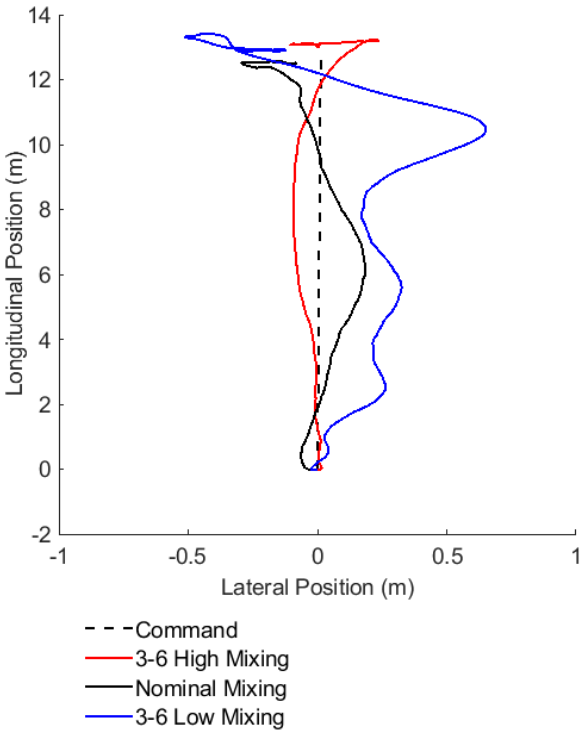

Figure 11. Example flight test data during the depart/abort MTE.

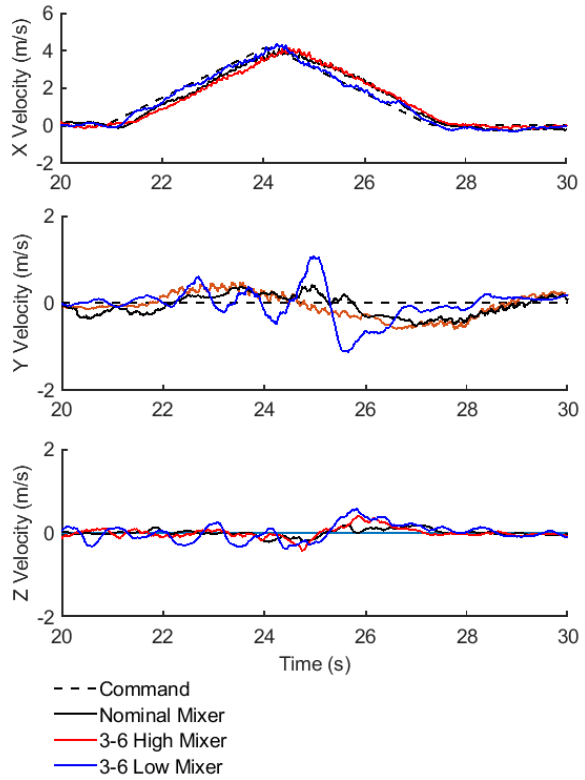

Figure 12. Example flight test velocity tracking during scaled depart/abort MTE.

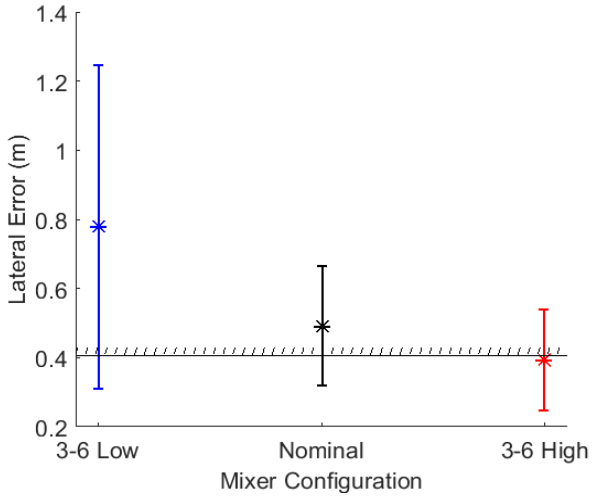

Figure 13. Mean and standard deviation of maximum lateral excursion during scaled depart/abort MTE.

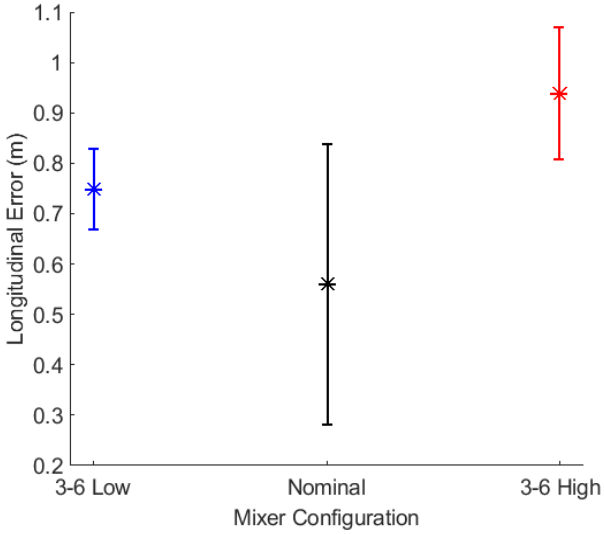

Figure 14. Mean and standard deviation of maximum longitudinal error during scaled depart/abort MTE.

FULL SCALE HEXACOPTER

The feasibility of these control allocation schemes to larger multirotor helicopters was studied at a conceptual design level using the tools and processes of [11, 23]. For the larger multirotor case, a 6-passenger (1,200-lb payload) hexacopter design (Figure 15 and Table 9) envisioned for an urban air mobility (UAM) application was explored.

A high-level open-loop block diagram representation of the control allocation matrix and bare-airframe is shown in Figure 16. Matrix T_{DN} mixes individual control-axes commands into rotor speed commands (relative to a speed reference) into individual engine speed controllers (ESCs). A difference between larger-scale and small UAS multirotor vehicles is that ESC loops must be synthesized simultaneously with the outer feedback loops (Figure 17) to ensure handling qualities requirements are realized with optimal engine usage.

Table 9. UAM hexacopter basic characteristics.

Parameter	**Value**
Design Gross Weight (lb)	6509
- Payload	1200
- Weight Empty	5299
- Operating Weight	5309
Number of Rotors	6
Design Disk Loading (lb/ft²)	3.0
Number of Blades	3
Rotor Radius (ft)	10.7
Solidity, thrust-weighted	0.055
Flapping Frequency (/rev)	1.03
Lock Number	4.61
Moments of Inertia (slug ft²)	
- I_{xx}	8385
- I_{yy}	18866
- I_{zz}	23291
Rotor Moment of Inertia (slug ft²)	109.2
SLS Power Available per engine (hp)	130.4

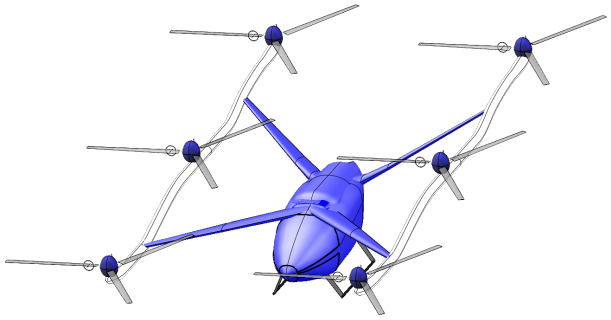

(a)

(b)

Figure 15. (a) Conceptual 6-passenger UAM hexacopter and (b) rotor numbering scheme.

It should be noted that the UAM hexacopter rotors are distributed in two straight lines on either side of the fuselage, rather than equally spaced like the University of Portland hexacopter.

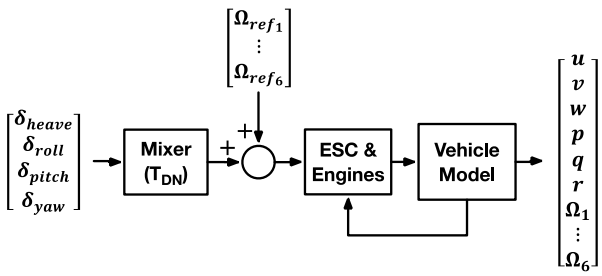

Figure 16. Mapping between control-axes commands and vehicle response.

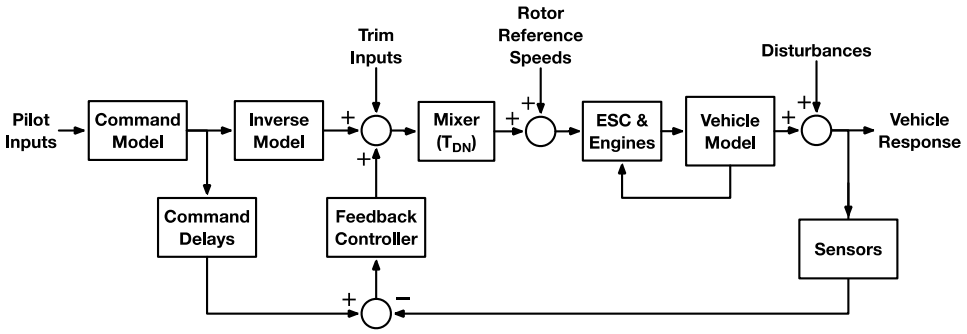

Figure 17. Model-following control system architecture with inner-loop ESC.

The nominal control allocation matrix T_{DN} was defined such that:

$$\begin{bmatrix}\Omega_{cmd_1}\\ \Omega_{cmd_2}\\ \Omega_{cmd_3}\\ \Omega_{cmd_4}\\ \Omega_{cmd_5}\\ \Omega_{cmd_6}\end{bmatrix} = \left(\frac{\pi}{30}\right)\begin{bmatrix}100 & -50 & -50 & 100\\ 100 & 50 & -50 & -100\\ 100 & -50 & 0 & -100\\ 100 & 50 & 0 & 100\\ 100 & -50 & 50 & 100\\ 100 & 50 & 50 & -100\end{bmatrix}\begin{bmatrix}\delta_{heave}\\ \delta_{roll}\\ \delta_{pitch}\\ \delta_{yaw}\end{bmatrix} + \begin{bmatrix}\Omega_{ref_1}\\ \Omega_{ref_2}\\ \Omega_{ref_3}\\ \Omega_{ref_4}\\ \Omega_{ref_5}\\ \Omega_{ref_6}\end{bmatrix} \quad (20)$$

where $\Omega_{ref_1} = \Omega_{ref_2} = \Omega_{ref_3} = \Omega_{ref_4} = \Omega_{ref_5} = \Omega_{ref_6} = \Omega_{ref}$ such that reference tip speed $\Omega_{ref}R = 550\ \text{ft/s}$. Off-nominal control allocation cases analyzed were defined by:

$$T_{DN} = \left(\frac{\pi}{30}\right)\begin{bmatrix}125 & -50 & -50 & 100\\ 125 & 50 & -50 & -100\\ 50 & -50 & 0 & -100\\ 50 & 50 & 0 & 100\\ 125 & -50 & 50 & 100\\ 125 & 50 & 50 & -100\end{bmatrix}_{3-4\ High} \quad (21)$$

and

$$T_{DN} = \left(\frac{\pi}{30}\right)\begin{bmatrix}75 & -50 & -50 & 100\\ 75 & 50 & -50 & -100\\ 150 & -50 & 0 & -100\\ 150 & 50 & 0 & 100\\ 75 & -50 & 50 & 100\\ 75 & 50 & 50 & -100\end{bmatrix}_{3-4\ Low} \quad (22)$$

Trim rotor speed and power required in hover for the hexacopter are shown in Table 10. To allow for easier examination of potential compressibility limits, rotor speeds are presented as tip speed. For reference, 550 ft/s tip speed corresponds to a rotor speed of 51.3 rad/s (or 489.5 RPM). All trim rotor speeds were found to be lower than the reference speed, which implies a negative trim δ_{heave} setting. Holding the trim setting constant at this negative value had the effect of reducing the rotor speeds for larger control allocation gains, which was contrary to the experience from the UP Hexacopter that does not use a reference trim RPM bias term. The aircraft had a slight (0.8 ft) forward CG offset, which explains the difference in speeds between the front and rear rotors.

Overall, changes in rotor speeds for the off-nominal control allocations were less than 6% for the UAM hexacopter. In contrast, The UP hexacopter has differences in speed from the low to high-speed trim motors of around 40%. The reason that the differences are much smaller here, as compared to the UP Hexacopter, is that this vehicle has a small power margin, resulting in only a 6% difference, at most, in the trim speed of the motors relative to the nominal case before Maximum Continuous Power (MCP) was reached on at least one motor pair. So, for the full-scale configuration, the differences in the rotor speeds are consistent with the differences in the thrust control derivatives in Table 11 for the individual rotors, remembering that $T \propto \Omega^2$. The same trends are seen as in the UP hexacopter - motors trimmed at higher RPM have higher thrust control derivatives and motors trimmed at lower RPM have lower thrust control derivatives.

Table 10. UAM hexacopter hover trim rotor speeds and power required UAM hexacopter.

Rotor Number	Nominal Mix		3-4 High		3-4 Low	
	Tip Speed (ft/s)	Power (%MCP)	Tip Speed (ft/s)	Power (%MCP)	Tip Speed (ft/s)	Power (%MCP)
1	503	93	489	85	517	100
2	503	93	489	85	517	100
3	492	87	521	102	463	75
4	492	87	521	102	463	75
5	481	83	465	78	495	88
6	481	83	465	78	495	88
Total		457.6 hp		461.1 hp		457.6 hp

Table 11. UAM hexacopter thrust control derivatives (T_Ω in lb/(rad/s)).

Rotor Number	Nominal	3-4 High		3-4 Low	
	Derivative	Derivative	Difference	Derivative	Difference
1	43.7	44.6	–3.04%	47.3	2.82%
2	43.7	44.6	–3.04%	47.3	2.82%
3	43.7	46.9	6.60%	40.9	–6.91%
4	43.7	46.9	6.60%	40.9	–6.91%
5	43.7	42.2	–3.38%	45.1	3.12%
6	43.7	42.2	–3.38%	45.1	3.12%

Table 12. UAM hexacopter roll and pitch stability and control derivatives.

Mixer	L_p	$L_{\delta_{roll}}$	$\left\lvert\frac{L_p}{L_{\delta_{roll}}}\right\rvert$	M_q	$M_{\delta_{pitch}}$	$\left\lvert\frac{M_q}{M_{\delta_{pitch}}}\right\rvert$
Nominal	–1.31	2.22	0.589	–1.49	–1.31	0.881
3-4 High	–1.31	2.22	0.589	–1.45	–1.27	0.875
3-4 Low	–1.31	2.22	0.593	–1.53	–1.35	0.884

A comparison of the primary roll and pitch stability and control derivatives (Table 12) shows only very small differences in the dynamics between the three control allocation cases might be attainable for the full-scale configuration with the power margins as currently designed. Because of the configuration of the roll axis with equivalent lateral offsets for all motors, the low and high thrust motors cancel each other out. In the pitch axis with the 3-4 Low configuration, there is some effect of the higher thrust derivative since motors 1,2,5, and 6 are all operating at elevated RPM, and therefore generate slightly more pitching moment. However, this is small because the thrust derivative differences are small compared to the nominal mixer.

Power required, being $P_{req} \sim \mathcal{O}(\Omega^3)$, varied more significantly for each rotor pair with the control allocation. Rotor pairs 3 and 4, and 1 and 2 required about 87–89 hp (MCP = 87.0 hp) for the 3-4 High and 3-4 Low off-nominal allocation cases, respectively. Without increasing the engine rated power, both off-nominal control allocation schemes mark the effective allocation limits for continuous operation for those rotor pairs. The 3-4 Low configuration, for example, does not require more power in total, but does operate the 1-2 motors at the MCP limit, which could be tolerated for short periods of time in a situation that warranted improved pitch tracking. However, in this case, the 2-3% improvement in pitch derivatives is likely not sufficient to significantly increase trajectory tracking capability, so may not be worth the additional complexity.

Optimal heave, roll, pitch, yaw and ESC loop feedback gains for the control system model-following architecture shown in Figure 17 were synthesized to minimize engine usage (actuator RMS), while satisfying basic stability and disturbance rejection requirements (Figure 18). Optimization of the control gains for the nominal mixer was performed using CONDUIT®. The optimization process rendered solutions with ESC response times on the order 0.6 s,

as defined by the rise time between 10 to 90% of the peak step response. Roll and pitch rate responses for the three control allocation cases are shown in Figure 19 with the coupled ESC/rotor dynamics now defined. As expected from the small variations in the dynamic properties (Table 12), negligible differences were found in the Bode plots. The eigenvalues in Figure 20 confirm the small attainable differences in the lateral and longitudinal hovering cubic modes, where the trends overall are consistent with the UP hexacopter case but with smaller percent changes due to the smaller trim speed differences between the motor pairs.

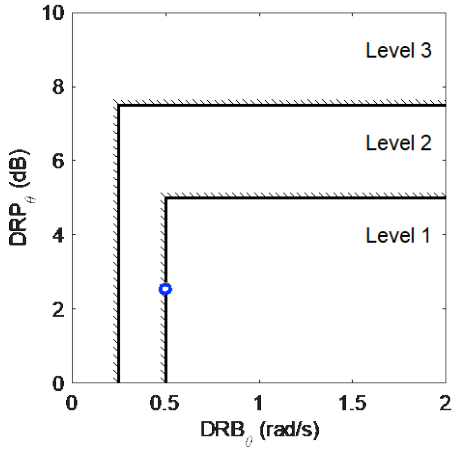

Figure 18. Pitch-axis feedback disturbance rejection specifications for nominal allocation.

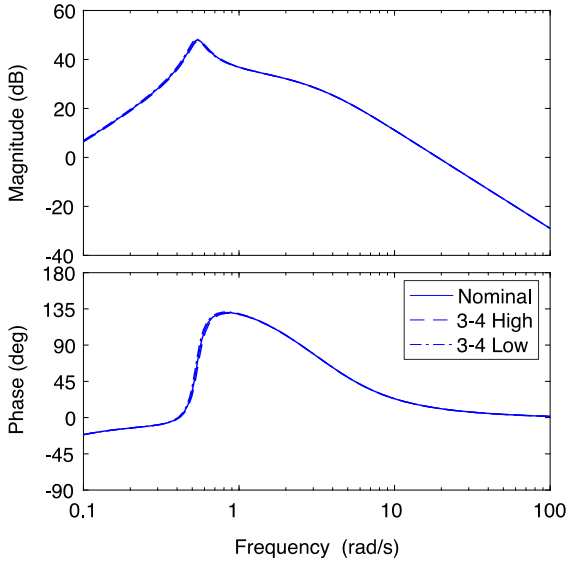

(a)

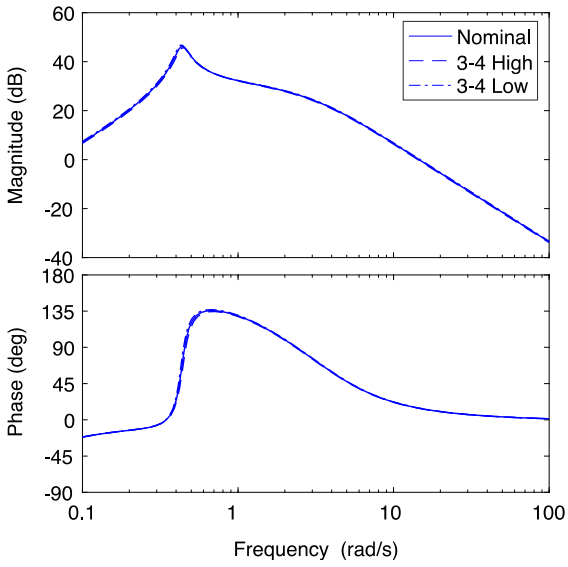

(b)

Figure 19. Frequency-response comparison: (a) roll rate and (b) pitch rate.

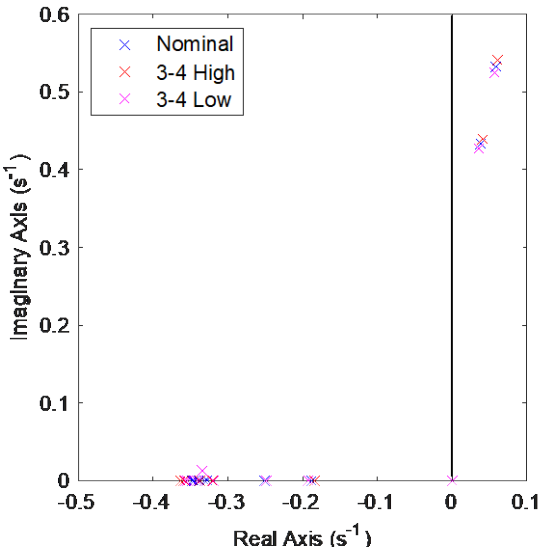

Figure 20. Bare-airframe eigenvalues comparison of the three control allocation cases.

DISCUSSION

Considering the trim and dynamic analysis results, together, for a small scale hexacopter vehicle with a large power margin, significant tracking differences on the order of 15% can be achieved in the roll axis. This comes at a tradeoff of increased overall power consumption and somewhat reduced performance in other control axes. For the UAM hexacopter, which is designed with much lower power margins for

efficiency, the benefits of varying the control allocation were not significant enough to offset the potential limitations of operating at MCP on some motors. The fundamental reason for this is because stability and control dynamics parameters for fixed-pitch rotors behave linearly with changes in the trim rotor speed, i.e.,

$$\frac{\partial T}{\partial w} \sim \mathcal{O}(\Omega) \quad \text{and} \quad \frac{\partial T}{\partial \Omega} \sim \mathcal{O}(\Omega) \tag{23}$$

but power grows cubically, i.e., $P_{req} \sim \mathcal{O}(\Omega^3)$. Therefore, small changes in rotor speed resulted in large changes in required power for that rotor when operating at higher speeds, reaching the power available for the engine models assumed. It is also noted that the rotor pairs operating at lower speeds have significantly reduced power, so the overall power consumed is only slightly increased in most cases.

Although this methodology had mixed results overall, there are still some important lessons learned. The trim RPM can significantly affect the handling qualities of the vehicle, and this should be considered when developing a multicopter, especially if its weight is expected to change dramatically – for example on multicopters designed to carry heavy cargo. The mass will vary significantly when dropping off cargo, and therefore the control derivatives and damping terms could vary significantly, not only due to inertial change but also because trim RPM will be reduced significantly on all motors. However, full-scale loaded passenger vehicles, like the conceptual UAM Hexacopter presented herein, operate with a lower power margin for efficiency because the weight and cost of the motors increase significantly as more power is required. In summary, the method presented herein could be used to an advantage in situations where increased tracking in a certain axis is needed, if the power margin is sufficient to allow these off-nominal operations.

CONCLUSION

This paper has evaluated the effect of off-nominal mixing to allocate power to multicopter rotors in a non-equal distribution across the motor pairs at hover/low-speed. The trim rotor speed of the motor pairs was varied to change the flight dynamics of the vehicle to increase control derivative and mode frequencies in certain axes (e.g. roll), at the cost of reduced control power and increased time constant in the other axes (e.g. pitch). This trade-off has been validated in flight test for a small hexacopter. Similar trends were found for a full-scale multicopter, but with less dramatic results due to the limited power margin which limited the off-nominal distribution of power between the motor pairings. Some key conclusions are:

1. Off-nominal control mixing can change the control effectiveness and plant dynamic modes due to the trim RPM which affects the handling qualities characteristics.
2. The effects on the flight dynamics were validated for a small hexacopter in flight test.
3. These plant variations can be exploited to improve disturbance rejection bandwidth for a small hexacopter
4. Evaluation of trajectory tracking maneuvers show that improved tracking can be achieved with off-nominal mixing, by about 10-15 % for a small hexacopter.
5. These effects are observed in larger multicopter simulation, but due to smaller power margin, the effects are less dramatic, resulting in changes on the order of 2-4%.

AKNOWLEDGEMENTS

This research was supported in part through NASA and Oregon Space Grant Consortium, cooperative agreement 80NSSC20M0035.

REFERENCES

[1] S. Withrow-Maser, C. Malpica and K. Nagami, "Multirotor configuration trades informed by handling qualities for urban air mobility applications," in *76th Annual Vertical Flight Society International Forum* , Virginia Beach, VA, 2020 .

[2] W. Johnson, C. Silva and E. Solis, "Concept Vehicles for VTOL Air Taxi Operations," in *AHS Technical Conference on Aeromechanics Design for Transformative Vertical Flight*, San Francisco, CA, 2018.

[3] R. Niemiec, F. Gandhi, M. Lopez and M. Tischler, "System Identification and Handling Qualities Perdictions of an eVTOL Urban Air Mobility Aircraft Using Modern Flight Control Methods," in *76th Annual Vertical Flight Society International Forum* , Virginia Beach, VA, 2020.

[4] A. Walter, M. McKay, R. Niemiec, F. Gandhi and C. Ivler, "Handling Qualities Based Assessment of Scalability for Variable-RPM Electric Multi-Rotor Aircraft," in *75th Vertical Flight Society Annual Forum*, Philadelphia, PA, May 13-16, 2019.

[5] J. Monterio, L. Fernadno and L. Hsu, "Optimal Control Allocation of Quadrotro UAVs Subject to Actuator Constrtants," in *American Control Conference, IEEE*, Boston, MA, 2016.

[6] G. Falconi and H. Florian, "Adaptive Fault Tolerant Control Allocation for a Hexacopter System," in *American Control Conference, IEEE*, Boston, MA, 2016.

[7] M. Saied, B. Lussier, I. Fantoni, H. Shraim and C. Fancis, "Active versus Passive Fault-Tolerant Control of a Redundant Mulitrotor UAV," *Aeronautical Journal, Royal Aeronautical Society,* vol. 124, no. 1273, pp. 385-408, 2019.

[8] G. Ducard and M. Hua, "Discussion and Practical Aspects on Control Allocation For a Multi-Rotor Helicopter," *International Archives of the Photogrammetry, Remote Sensing and Spatial Information Science, ISPRS Zurich 2011 Workshop,* Vols. XXXVIII-1/C22, 2011.

[9] D. Hackenberg, "AAM Mission Strategy: NASA Adanced Air Modbility MIssion," in *AAM Ecosystem Working Groups Meetings*, March 23, 2020.

[10] C. Ivler, K. Troung, K. D., J. Otomize, P. D., N. Gowans and M. Tischler, "Development and Flight Validation of Proposed Unammed Aerial System Handling Qualiites Requirements," in *VFS 76th Annual Forum and Technical Display*, October, 2020.

[11] C. Malpica and S. Withrow-Maser, "Handling Qualities Analysis of Blade Pitch and Rotor Speed Controlled eVTOL Quadrotor Concepts for Urban Air Mobility," in *VFS International Powered Lift Conference*, San Jose, CA, January 2020.

[12] J. Downs and e. al, ""Control system development and flight test experience with the MQ-8B fire scout vertical take-off unmanned aerial vehicle (VTUAV)," in *American Helicopter Society International 63rd Annual Forum*, Virginia Beach, VA, 2006.

[13] C. Ivler, K. Russell, A. Gong, T. Berger, Lopez and M. J.S., "Toward a UAS Handling Qualities Specification: Development of UAS-Specific MTEs," in *Vertical Flight Society 78th Annual Forum*, Dallas-Fort Worth, TX, May 2022.

[14] anon, "ardupilot.org," [Online]. Available: ardupilot.org/copter/index.htm.

[15] anon, "Mission Planner," [Online]. Available: ardupilot.org/planner/index.htm.

[16] C. Ivler, E. Rowe, J. Martin, M. Tischler and M. Lopez, " System Identification Guidance for Multirotor Aircraft: Dynamic Scaling and Test Techniques.," in *Vertical Flight Society International Forum*, Philadelphia, PA, May, 2019.

[17] R. Chen, "An Exploratory Invesitgation of the Flight Dynamics Effects of Rotor RPM Variations and Rotor State Feedback In Hover," NASA TM 103968, NASA Ames Reserach Center, September 1992.

[18] M. Lopez, M. Tischler, O. Juhasz, A. Gong and F. Sanders, "Development of a Reconfigurable Multicopter Flight Dynamics Model from Flight Data Using System Identification," in *8th Biennial Autonomous VTOL Technical Meeting*, Mesa, AZ, January 29-31, 2019.

[19] C. Ivler, R. Niemiec, F. Gandhi and F. Sanders, "Multirotor Electric Aerial Vehicle Model Validation with Flight Data: Physics-Based and System Identification Models," in *Vertical Flight Society Annual Forum*, Philadephia, PA, May, 2019.

[20] M. Tischler and R. Remple, Aircraft and Rotorcraft System Identification: Engineering Methods with Flight Test Examples, Reston, VA: AIAA Education Series, 2012.

[21] R. Niemiec and F. Gandhi, "Development and Validation of the Rensselaer Multicopter Analysis Code (RMAC): A Physics-Based Comprehensive Modeling Tool," in *Vertical Flight Society 75th Annual Forum*, Philadelphia, PA, May 2019.

[22] M. Tischler, T. Berger, C. Ivler, K. K. Cheung and J. Soong, Practical Methods for Aircraft and Rotorcraft Flight Control Design: an Optimization Based Approach, Reston, VA: AIAA, 2017.

[23] S. Withrow-Maser, C. Malpica and K. Nagami, "Impact of Handling Qualites on Motor Sizing for Multirotor Aircraft with Urban Air Moblity Missions," in *Vertical Flight Society 77th Annual Forum*, Virtual , May, 2021.